

Research Article

Numerical gradient-index design for coherent mode conversion

Di Lin* and James R. Leger

Department of Electrical and Computer Engineering,
University of Minnesota, Minneapolis, MN, USA

*Corresponding author
e-mail: linx0284@gmail.com

Received April 2, 2012; accepted May 4, 2012

Abstract

We present a numerical gradient-index (GRIN) design methodology for application in coherent mode conversion. Within the framework of geometric optics, a one-to-one correspondence between the field description and the ray description of the propagating beam is established using optical path lengths and the conservation of energy within a bundle of rays. A family of ray paths is chosen to transform the initial ray distribution into a target ray distribution. The specified ray paths are used to calculate the index profile of the GRIN structure required to effect the gradual transformation from the input beam to the desired output beam. We demonstrate our approach with a GRIN structure design that converts a Gaussian beam into a flat-top beam.

Keywords: beam shaper; GRIN; inhomogeneous; mode conversion; ray trace.

1. Introduction

Mode conversion optics is useful in a variety of coherent optical systems. For example, the Gaussian irradiance of a stable spherical mirror laser resonator mode is not always ideally matched to the application at hand, and conversion to another shape can be desirable. In particular, it can be shown that the irradiance of a light beam at the focal plane of a lens is maximized when the lens pupil is illuminated by a laser beam that is uniform in both amplitude and phase [1]. Alternatively, applications such as holography and laser Doppler velocimetry require uniform illumination in the near field, whereas laser radar systems often require uniform far-field illumination [2]. A second area where beam shaping finds utility is in the area of coherent laser beam combining [1, 3]. A special optical system is generally used to establish phase coherence across a laser array. The resultant beam then consists of a single spatial mode (because all lasers are locked in phase), but often maintains the shape of the original array. For many practical applications, this mode shape must be converted into a more useful format (such as a Gaussian or uniform distribution) to

take full advantage of the spatial coherence of the laser mode. Indeed the highest radiance (defined as power per unit area per unit solid angle, where the area and solid angles are defined in terms of second-order intensity moments) is obtained when the mode is converted into a Gaussian distribution [4].

Over the years, many techniques have been developed to change the shape of coherent modes [5, 6]. These include aspheric refractive optics [7, 8], spherical refractive optics with specific amounts of spherical aberration [9], reflective optics [10, 11], holographic methods [12], polarization-based techniques [13, 14], and grating superposition techniques [15]. One method that has not been as well explored is the use of gradient-index (GRIN) technology for beam shaping. In a GRIN structure, the index of refraction of a material is changed in a specified manner as a function of location within the material. With the recent advances in arbitrary GRIN fabrication techniques, it is reasonable to assess whether GRIN structures can perform arbitrary coherent mode conversion. A selection of these techniques include: slurry-based three-dimensional (3D) printing [16], neutron irradiation [17], various methods of chemical vapor deposition [18–22], ion exchange [23, 24], ion stuffing [25], and the sol-gel method [26–28]. Each fabrication technique is subject to its own limitations; the primary limiting characteristics of a particular process pertaining to our application of GRIN materials are the physical depth into which the refractive index of the material can be modified (depth of the gradient), the maximum change in the refractive index and most importantly, the type of index profile the process can achieve. As the current limits to the depth of the gradient are generally on the order of several millimeters, the advent of microscale GRIN mode converters in the realm of microoptics is foreseeable in the near future. Previous researchers have explored GRIN structures as replacements for aspheres in a more traditional Gaussian-to-flat-top converter [29]. In this paper, however, we explore the promise of GRIN for more generalized beam shaping, establish a design procedure for an arbitrary redistribution of irradiance, and propose several optimization strategies. Potential advantages of GRIN optics for generalized beam shaping include elements with planar input/output surfaces for more convenient interfacing to lasers and fibers, high optical efficiency, short device lengths, convenient integration of passive optics with mechanics and packaging, and convenient fabrication of microoptics and arrays.

2. Ray description of optical beams

In an optical medium where the refractive index can vary with position, geometric optics is often used to calculate the trajectory of a ray propagating through the structure. We assume

the scalar wave equation can be satisfied by a trial solution of the form:

$$\psi(\vec{r}, t) = A(\vec{r})e^{i[k_0 S(\vec{r}) - \omega t]} \quad (1)$$

where $k_0 = \frac{2\pi}{\lambda_0}$ is the wavenumber in free space. Substituting

Eq. (1) into the scalar wave equation and neglecting the second-derivative term ∇^2 yields the Eikonal equation:

$$|\nabla S(\vec{r})|^2 = n^2(\vec{r}) \quad (2)$$

The trial solution in Eq. (1) is a good approximation provided that:

$$\left| \frac{\lambda_0}{n^2(\vec{r})} \nabla n \right| \ll \sqrt{32}\pi \quad (3)$$

This condition defines a ‘slowly varying’ optical medium [30] and must be satisfied in our designs where $n(\vec{r})$ is continuous in order for geometric optics to be valid.

The framework of geometric optics requires a one-to-one correspondence between the field description and ray description of an optical beam. Once this relationship has been established, the Eikonal equation, Eq. (2), and its associated ray equation, can be used in conjunction with the intensity law of geometric optics to compute the propagation of the optical beam inside a known optical medium (neglecting diffraction). This is known as the direct problem of ray tracing. Our design methodology addresses the inverse problem of determining the refractive index profile of an optical medium using defined ray trajectories. Both analytical and numerical solutions to the inverse problem have been studied in [31]. The present study prescribes a simpler numerical method to solve the inverse problem for application in coherent mode conversion. By appropriate application of the Eikonal and ray equations, the refractive index distribution required to guide rays along prescribed trajectories can be calculated.

Recalling that radiant energy is conserved within a bundle of rays according to the geometric optics intensity law for propagation of energy, one can relate ray density to the irradiance of an optical beam. Rhodes and Shealy used this law to calculate the redistribution of irradiance by two aspheric refractive surfaces. Starting with an input beam represented by uniformly spaced rays of variable irradiance, they calculated the radial distance (from the axis of symmetry) of each ray at the output aperture [7]. The irradiance of the optical beam is represented by the local ray density and its phase by the collective optical path length (OPL) of the ray distribution.

Consider a radially symmetric optical beam where the ray height y represents the radial distance of the ray from the axis of symmetry. To determine the positions of the rays in the ray description of the optical beam, a stepwise approximation to the integrated irradiance function $\varphi(y)$ can be employed, where $\varphi(y_0)$ describes the total irradiance contained within $y < y_0$ in a plane that is orthogonal to the axis of symmetry. Naturally, $\frac{d\varphi}{dy}$ describes the irradiance profile of the optical

beam in that plane along the radial direction. The integrated irradiance function is particularly convenient when assigning variable amounts of flux to each ray in the ray description. Because this ray description is based on energy conservation, each ray represents a set amount of flux across a unit surface area lying perpendicular to the ray. Thus, ray angles must be accounted for when calculating the irradiance of the optical beam in a given plane from its ray description and vice versa. Conversely, given a ray distribution in a particular plane, integrating the irradiance of each successive ray as one moves away from the axis of symmetry yields a stepwise approximation to the integrated irradiance function. The irradiance profile of the optical beam in that plane can then be obtained by differentiating the interpolated version of the integrated intensity function. An example of a ray distribution calculated from the integrated irradiance function of a Gaussian irradiance profile is shown in Figure 1.

The phase distribution of the optical beam is represented by the collective OPLs of the ray distribution. The OPLs of all rays must be identical along geometrical wavefronts. In addition, ray directions must be consistent with the shape of the geometrical wavefront because rays are always perpendicular to the local wavefront. This holds true for continuous distributions of the refractive index.

3. Solving for the refractive index

In this section, we address the following question: Given a particular coherent mode transformation, is it always possible, subject to the limitations of ray optics, to find a GRIN distribution that will perform the desired transformation? To answer this, we consider a refractive index distribution $n(\vec{r}) = n(x, y)$ used for a two-dimensional irradiance redistribution where x denotes the propagation axis. Suppose there is a ray family $Y(x, h)$ that contains all the rays in the conversion mapping such that evaluating $Y(x, h)$ at a particular value of h singles out a ray path. If $Y(x, h)$ is completely specified, solving a first-order partial differential equation will determine the refractive index profile of the GRIN structure needed to effect the conversion.

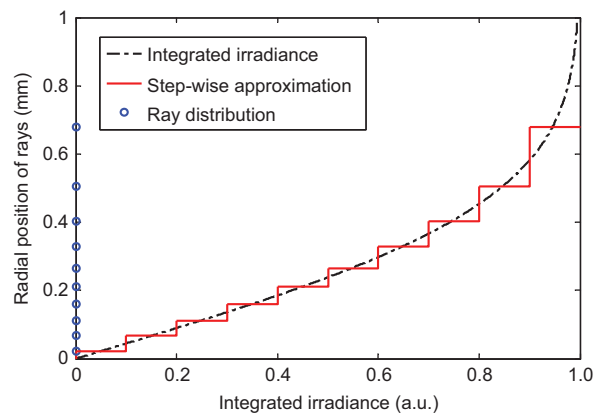


Figure 1 Ray distribution calculation using a stepwise approximation to the integrated irradiance function for a Gaussian irradiance profile. Each ray represents the same amount of radiative flux.

The complete derivation is available in [31]. We will briefly outline the solution starting with the ray equation, Eq. (4).

The equation governing the ray path in an inhomogeneous optical medium follows directly from the Eikonal equation, Eq. (2), and is given by:

$$\frac{d}{ds} \left(n(\vec{r}) \frac{d\vec{r}}{ds} \right) = \vec{\nabla} n(\vec{r}) \quad (4)$$

where ds is the arc length along the ray path, \vec{r} is the position vector of a point on the ray trajectory, and $n(\vec{r})$ is the index of refraction at position \vec{r} . If all rays in $Y(x, h)$ follow trajectories where the ray heights y are single-valued functions of position along the propagation axis, i.e., $y=y(x)$, then Eq. (4) can be rewritten as:

$$\frac{dy}{dx} \frac{\partial w}{\partial x} + \frac{\frac{d^2 y}{dx^2}}{1 + \left(\frac{dy}{dx} \right)^2} = \frac{\partial w}{\partial y} \quad (5)$$

where $w = \ln(n(x, y))$. This can be conveniently expressed in the form of a first-order partial differential equation, which can be reduced to the following system of ordinary differential equations using the method of characteristics:

$$\frac{dx}{dy} = - \frac{dY}{dx} \quad (6a)$$

$$\frac{dw}{dy} = \frac{\frac{d^2 Y}{dx^2}}{1 + \left(\frac{dY}{dx} \right)^2} \quad (6b)$$

where the single ray paths $y=y(x)$ have been generalized to the entire ray family $Y(x, h)$ in the conversion mapping. The first equation simply describes the geometrical wavefronts that lie perpendicular to the ray paths, whereas the second equation solves for the index of refraction along these wavefronts. A solution for $n(x, y)$ exists if the ray family $Y(x, h)$ satisfies the following conditions [31]:

- $Y(x, h)$ has continuous second partial derivatives $\frac{d^2 Y}{dx^2}$.
- $Y(x, h)$ has continuous second mixed partial derivatives $\frac{d}{dh} \left(\frac{dY}{dx} \right)$.
- $Y(x, h)$ has continuous first partial derivatives $\frac{dY}{dh}$ and $\frac{dY}{dx} \neq 0$.

The ray equation, Eq. (4), also allows us to solve for the gradient of the refractive index $\vec{\nabla} n(\vec{r})$ along any particular ray path. However, the gradient calculated from the entire ray family $Y(x, h)$ will not be a conservative field without imposing the proper constraints, suggesting that a solution $n(\vec{r})$ does not exist. To guarantee the existence of a solution in the gradient method, we must require all rays in $Y(x, h)$ to have identical OPLs along all possible geometrical

wavefronts. Thus, subject to the aforementioned conditions, it is always theoretically possible to convert any coherent mode into any other coherent mode with a properly designed GRIN element.

4. Numerical implementation

Although the system of ordinary differential equations in Eq. (6) can be used in principle to determine the refractive index along the geometrical wavefronts of the ray family $Y(x, h)$, it is possible to use a more straightforward method to calculate this index profile using only the wavefronts. The Eikonal equation, Eq. (2), provides an intuitive way of justifying this approach and can be written in the form:

$$\vec{\nabla} S(\vec{r}) = n(\vec{r}) \hat{s} \quad (7)$$

where a constant contour of $S(\vec{r})$ describes a geometrical wavefront of constant OPL and \hat{s} is a unit vector lying perpendicular to the wavefront at position \vec{r} . Eq. (7) states that the product between the refractive index and arc length is responsible for an incremental increase in $S(\vec{r})$. This means the refractive index can be calculated easily with two different constant contours of $S(\vec{r})$. Therefore, rather than solving the system of ordinary differential equations in Eq. (6), it is possible to obtain the index profile of the GRIN structure by constructing wavefronts from just a small number of sampling rays and performing elementary calculations. We will denote the sampling rays as $Y(x, h_s)$, where a discrete value of h_s corresponds to a particular sampling ray.

Our numerical method starts by defining the initial and final positions of the sampling rays in $Y(x, h_s)$ from the input and output optical beams. Owing to the discrete nature of rays, the initial and final ray distributions are obtained from a stepwise approximation to an integrated intensity function $\varphi(y)$. The initial and final directions of the rays in $Y(x, h_s)$ can be calculated straightforwardly by differentiating the phase (with respect to y) in their irrespective field distributions (as rays are always perpendicular to the local wavefront). In addition, the OPL of the rays in $Y(x, h_s)$ must be specified (up to an arbitrary constant) in the input and output ray distributions and be consistent with the phase distribution of the optical beam in those planes. Finally, a predetermined amount of radiative flux is assigned to each ray such that the energy propagating at the specified ray angles yields the proper amount of irradiance in the plane of interest. As irradiance is represented by local ray density in the prescribed ray description, there tends to be an excessive number of rays in regions of high irradiance and insufficient rays in regions of low irradiance. This becomes problematic when we encounter irradiance profiles with high contrast. One possible solution is to insert additional sampling rays of variable radiative flux into the sampled conversion mapping $Y(x, h_s)$ in a manner that does not affect the irradiance profile of the input and output beams. Two different sampling ray paths $Y(x, h_s)$ belonging to the same ray family $Y(x, h)$ are shown in Figure 2.

Each ray in the output distribution is paired up with a ray in the input distribution in a manner that is consistent with

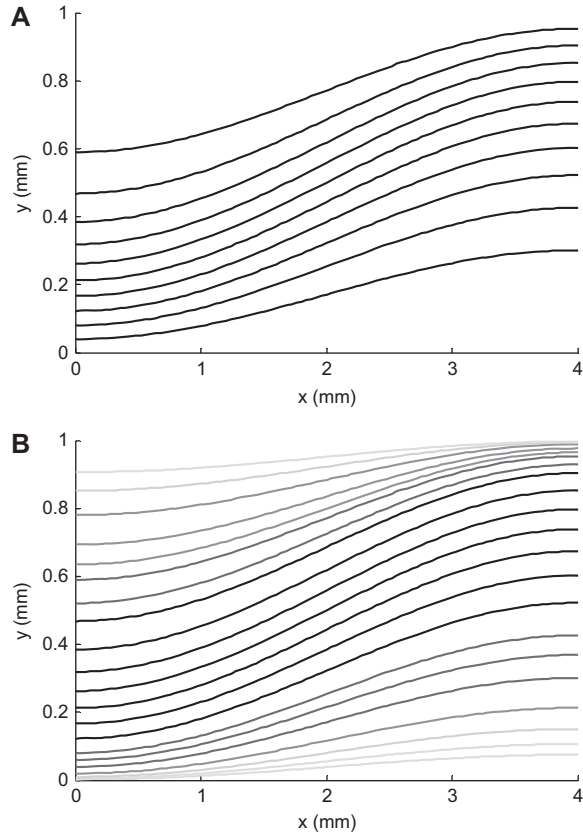


Figure 2 (A) Ray trace of a high contrast irradiance profile, showing sparse data points in low irradiance areas. (B) Additional sampling rays are inserted to overcome sparse sampling. Lighter shades of the ray path indicate decreasing amounts of radiative flux for the particular ray.

energy conservation and does not result in any intersecting rays (intersection of ray trajectories violates the second condition that guarantees the existence of a solution to the inverse problem). Each pair is assigned a ray path $Y(x, h_s)$ whose height Y and slope $\frac{dY}{dx}$ are constrained in the input and output planes. An infinite number of choices exist for $Y(x, h_s)$ that will satisfy these constraints. However, requiring all ray paths in $Y(x, h_s)$ to follow the same functional form (e.g., a low-order polynomial) generally reduces the complexity of the design. Once the trajectories of the sampling rays have been chosen, extrapolation can be used to construct a family of wavefronts $X(y, l)$ that lie perpendicular to every ray in $Y(x, h_s)$. A discrete set of these constructed (or ‘sampling’) wavefronts, denoted by $X(y, l)$, is used to compute the refractive index profile responsible for the gradual evolution of the wavefront as the optical beam propagates through the GRIN structure.

The inverse problem of calculating the refractive index profile from the defined ray trajectories presents an infinite number of solutions. This is because solving the ordinary differential equations in Eq. (6) can only determine the refractive index profile up to an arbitrary function of the geometrical wavefronts [31]. In order to narrow the design down to a unique solution, the OPLs of the sampling wavefronts must be

specified. These values are completely arbitrary, provided that the change in OPL is monotonic as we follow the ray paths in one direction. The possibility of having discontinuities in the refractive index along these wavefronts is inconsequential for ray paths in $Y(x, h)$ (by application of Snell’s law) because the rays are always perpendicular to the plane of discontinuity.

The intersection between the ray paths $Y(x, h_s)$ and wavefronts $X(y, l)$, whose position is denoted by $\bar{r}(l_i, h_s)$, provide sample points where the OPL is known. This can be used to calculate the refractive index between two adjacent OPL sample points along a particular sampling ray using the OPL difference and arc length:

$$n(\bar{r}') = \frac{\phi(l_{i+1}, h_s) - \phi(l_i, h_s)}{\int_{\bar{r}(l_i, h_s)}^{\bar{r}(l_{i+1}, h_s)} dS} \quad (8a)$$

$$\bar{r}' = \frac{\bar{r}(l_{i+1}, h_s) + \bar{r}(l_i, h_s)}{2} \quad (8b)$$

where $\phi(l_i, h_s)$ is the OPL at $\bar{r}(l_i, h_s)$. This calculation is repeated for every pair of adjacent OPL sample points and the resulting data points for the refractive index are used to interpolate the overall refractive index profile of the GRIN structure.

5. Gaussian-to-flat-top GRIN design

To verify our approach, the design formula outlined in the previous section is used to calculate the refractive index profile of a GRIN structure that converts an input Gaussian beam into a circular output beam with uniform irradiance. The configuration is shown in Figure 3. The radial symmetry of this irradiance redistribution allows the problem to be treated using just one dimension in the transverse plane. However, the irradiance profile must scale linearly with radial distance from the axis of symmetry to account for the coordinate transformation.

As both the input and output beams have planar wavefronts in this particular design, all rays in the input and output ray distributions are parallel to the axis of symmetry. Cubic polynomials and half-period sinusoids are two potential functions to describe the ray paths $Y(x, h_s)$ in the conversion mapping. The choice between the two results in a slightly different refractive index profile in the design. We discuss this choice of mapping functions in a subsequent section. For this design, half-period sinusoidal ray paths are chosen for $Y(x, h_s)$, as shown in Figure 2. The geometric wavefronts $X(y, l)$ are

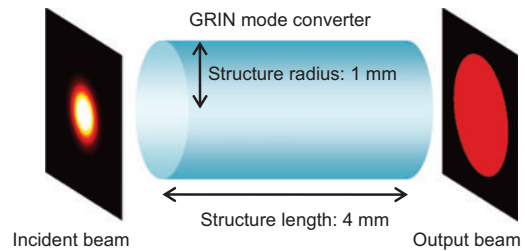


Figure 3 Diagram of a Gaussian-to-flat-top beam converter using a GRIN structure. Incident Gaussian beam width is 0.354 mm. Output beam radius is 1 mm.

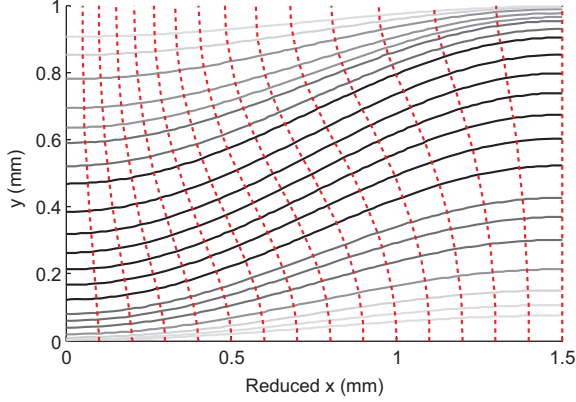


Figure 4 Extrapolated wavefronts from sample rays in the conversion mapping shown in Figure 2B. Note the length of the structure has been reduced to scale the x - and y -axes equally and preserve the orthogonality between rays and geometrical wavefronts in this figure.

constructed from $Y(x, h_s)$ and are depicted in Figure 4. The refractive index is set to a constant along the axis of symmetry; this constrains the OPLs of the sampling wavefronts. Using Eq. (8) to calculate the refractive index profile of the GRIN structure, the interpolated result is shown in Figure 5.

A forward ray trace is used to verify the design. Starting with the same irradiance distribution (represented using a smaller number of rays), each ray is traced through the GRIN structure using the ray equation, Eq. (4), to obtain the output ray distribution. A straightforward numerical implementation of the forward ray trace can be found in [32]. The irradiance and phase profile of the output beam is shown in Figure 6. The GRIN structure is shown to redistribute the irradiance profile of the Gaussian beam into a circular flat-top beam with a peak-to-valley OPL error (phase error) of $\lambda/16$ (assuming a wavelength of $1 \mu\text{m}$).

6. Design optimization

Modern fabrication techniques do not yet have the capability to produce GRIN structures with arbitrary $n(x, y, z)$. The issues

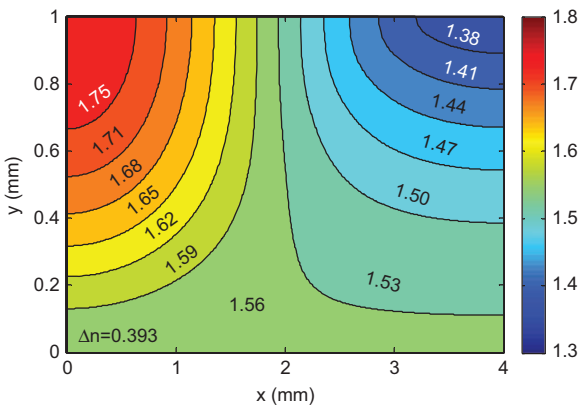


Figure 5 Refractive index profile of a non-optimized Gaussian-to-flat-top beam converter.

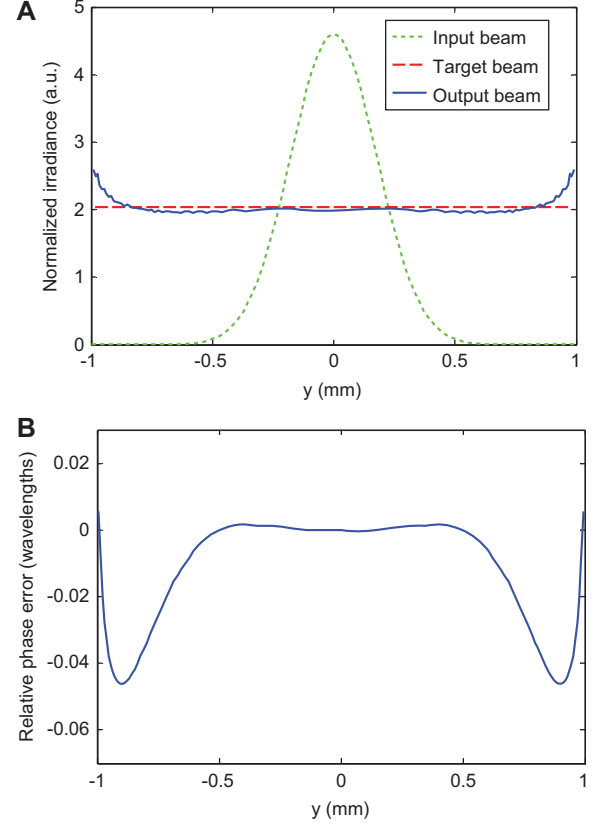


Figure 6 Ray trace through the mode converter structure designed to convert a Gaussian intensity to a radial flat-top intensity. (A) Input and output beam irradiance. (B) Relative phase error assuming a wavelength of $1 \mu\text{m}$.

associated with fabrication will often impose additional constraints in the design process. In particular, materials used for fabricating the GRIN structure limit the dynamic range of the refractive index profile, defined as $\Delta n = n_{\max} - n_{\min}$. Fortunately, there are several methods that can be used to reduce Δn in our design.

6.1. Method 1

If changes to the ray paths in the conversion mapping $Y(x, h)$ are not allowed, the minimum Δn of the GRIN structure can be determined from the maximum arc length ratio of the structure, α_{\max} , given by:

$$\alpha_{\max} = \max_i \left(\frac{\max_s ds_{i,s}}{\min_s ds_{i,s}} \right) \quad (9)$$

where $ds_{i,s}$ is the arc length between sampling wavefronts $X(y, l_i)$ and $X(y, l_{i+1})$ along the sampling ray corresponding to h_s in $Y(x, h_s)$. As the OPL is constant between any two adjacent wavefronts (or more generally, any two wavefronts), the arc length ratio can also be expressed as $\alpha_{\max} = \frac{n_{\min}}{n_{\max}}$. This reveals that the ratio of n_{\min} to n_{\max} is determined solely by

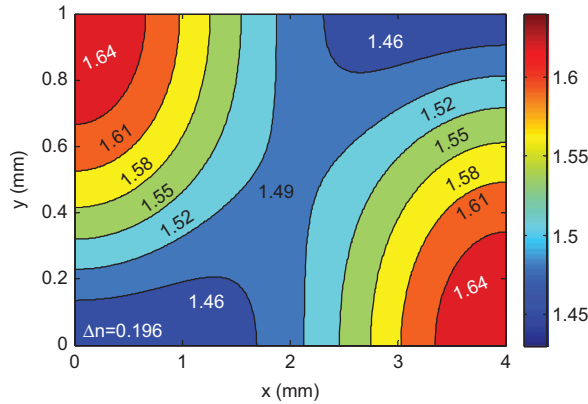


Figure 7 Interpolated refractive index profile for a Gaussian-to-flat-top beam converter after modifying the OPL of sample wavefronts to reduce Δn .

the maximum ratio between the maximum and minimum arc lengths between any two adjacent sampling wavefronts. After calculating the ratio in Eq. (9), we can modify OPLs of the sampling wavefronts accordingly to reduce Δn in the design (recall that these are arbitrary as long as the OPL is monotonically increasing as the optical beam propagates forward). Figure 7 illustrates the change in the refractive index profile from the GRIN mode converter calculated in Section 5 after the OPL of the sampling wavefronts $X(y, l_i)$ has been modified. As a general rule, the index profile should be kept as simple and smooth as possible (i.e., maintaining continuous second derivatives and mixed partial derivatives).

6.2. Method 2

If we were to allow changes in the conversion mapping $Y(x, h)$, more options become available for reducing Δn in the design. One possibility is to scale the output beam. Figure 8 shows the new conversion mapping after resizing the output beam to 55% of the input aperture, minimizing Δn for a Gaussian

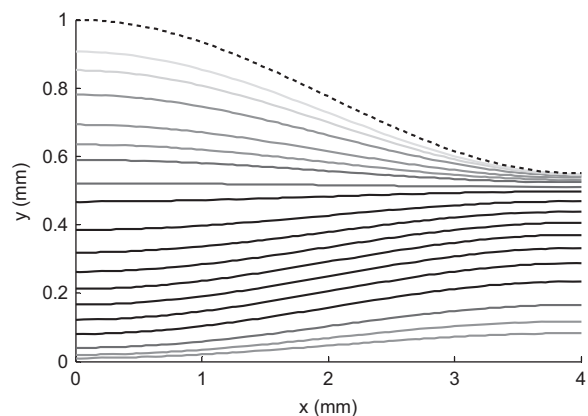


Figure 8 Conversion mapping after resizing the output beam to 55% of the input aperture (minimizes Δn for a Gaussian beam with an initial beam width of 0.354 mm). Dotted line shows the extent of the conversion mapping.

beam with a 0.354-mm beam width. This optimal condition was determined by calculating α_{max} for various output beam radii. An important observation is that the refractive index variation is no longer monotonic along the radial direction. Recall that all rays in the previous mapping were being guided away from the axis of symmetry by the GRIN material, allowing for a monotonic index with respect to radius. In the modified conversion mapping, rays near the edge of the structure are being guided towards the center, whereas rays in the center are being guided away from the center. Thus, a non-monotonic index profile is required. Figure 9A shows the resulting refractive index profile after resizing the output beam while keeping the refractive index constant along the axis of symmetry. The design in Figure 9B relaxes this constraint and further reduces Δn by incorporating Method 1 after resizing the output beam.

6.3. Method 3

Another possibility to reduce Δn in the design is to modify the functional form of the ray paths when changes to $Y(x, h)$ are permitted. In Section 5, half-wave sinusoids were used in the Gaussian-to-flat-top beam converter design. Figure 10 shows the change in the refractive index profile if the rays were to follow cubic polynomials instead of sinusoids, where the

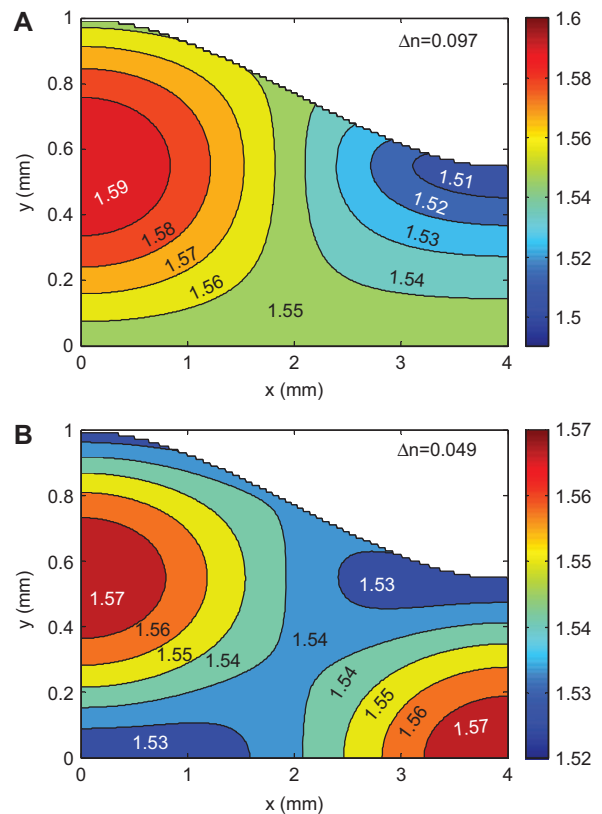


Figure 9 Interpolated refractive index profile for a Gaussian-to-flat-top beam converter. (A) Radius of the output beam optimized to 55% of its original size with no Optical path difference (OPD) optimization. (B) Radius reduced to 55% and OPD was optimized to minimize refractive index ratio. White on graphs indicates regions outside the conversion mapping.

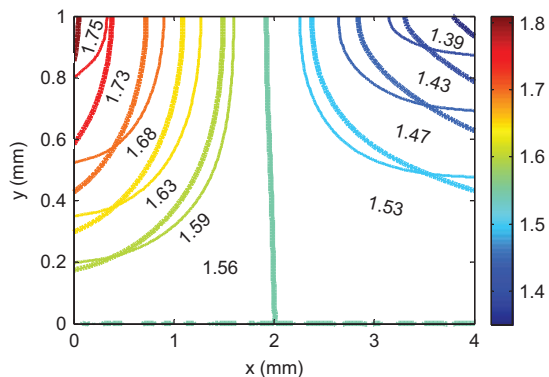


Figure 10 Refractive index comparison between cubic polynomials (thick contour lines) and half-wave sinusoids (thin contour lines) used as ray paths in the conversion mapping. The cubic polynomials result in a higher $\Delta n=0.487$, compared with the sinusoid solution of $\Delta n=0.393$.

other design parameters are as used to obtain the refractive index profile in Figure 5. In our simulations, the sinusoidal ray path resulted in a smaller index difference Δn . We hasten to add, however, that we have not proven the optimality of sinusoids. There may, in fact, be functions that are superior to sinusoids for this particular application. This aspect of the design method remains largely unexplored.

6.4. Method 4

A final method to reduce the index difference is to increase the device length. This is analogous to increasing the f -number of a conventional lens. Generally speaking, increasing the length of the GRIN structure will always reduce Δn . This is because as ray paths become more paraxial in the conversion mapping, adjacent sampling wavefronts become more parallel with respect to each other and the ratio in Eq. (9) is reduced. In the extreme limit where the structure is infinitely long, α_{max} approaches unity and n_{min} approaches n_{max} .

These optimization methods are not specific to Gaussian-to-flat-top design and can be generalized to more complex applications of GRIN coherent mode conversion. As should be apparent, all the optimization methods described above except lengthening the device generally result in a more complex structure. Specific fabrication methods may require the central ray to see a constant index. Alternatively, a non-monotonic refractive index profile (along the radial direction) may be difficult or impossible to fabricate given a specific technology. Thus, an overall optimization procedure must take fabrication constraints into account along with the index difference.

7. Conclusion

In response to the recent advances in GRIN fabrication technology, we have developed a simple numerical method for calculating the refractive index profile of a GRIN structure used for coherent mode conversion. Within the framework of

geometric optics, energy conservation was used to establish a general ray description of an optical beam. The conversion mapping could then be specified by choosing a family of ray paths. Under the appropriate conditions, the refractive index distribution that effects the mode conversion could be obtained by solving a partial differential equation or by using geometrical wavefronts. We described a simple approach based on wavefronts and demonstrated its effectiveness by designing a GRIN structure to convert an incident Gaussian beam into a circular flat-top beam. A forward ray trace simulation shows that the designed GRIN structure redistributes the irradiance of the incident beam as intended and produces the correct phase profile. In addition, several methods of reducing the dynamic range of the GRIN structure were also discussed. We have shown in our simulations that these GRIN devices are capable of redistributing the irradiance profile of an optical beam over extremely short propagation distances. The same applies for altering the shape of the wavefront in an optical beam. This feature is especially advantageous in the realm of microoptics where compact optical components are needed for integration in microsystems.

Author contributions

Di Lin was responsible for algorithm development, computer coding and design optimization. James R. Leger was responsible for project formulation, direction and consultation. Both Di Lin and James R. Leger were responsible for writing, reviewing and editing the manuscript.

References

- [1] J. R. Leger, in 'Surface Emitting Semiconductor Lasers and Arrays', Ed. by G. Evans and J. Hammer (Academic Press, New York, 1993) pp. 379–433.
- [2] W. B. Veldkamp and C. J. Kastner, *Appl. Opt.* 21, 345–356 (1982).
- [3] J. R. Leger, in 'Diode Laser Arrays', Ed. by D. Botez and D. Scifres (Cambridge University Press, Cambridge, 1994) pp. 123–179.
- [4] A. E. Siegman, *NATO Adv. Study Inst. Ser. B Phys.* 317, 13–28 (1993).
- [5] F. M. Dickey and S. C. Holswade, Eds., in 'Laser Beam Shaping: Theory and Techniques' (Marcel Dekker, New York, 2000).
- [6] J. R. Leger, in 'Microoptics', Ed. by H. P. Herzig (Taylor and Francis, London, 1996) pp. 223–259.
- [7] P. W. Rhodes and D. L. Shealy, *Appl. Opt.* 19, 3545–3553 (1980).
- [8] S. R. Jahan and M. A. Karim, *Opt. Laser Technol.* 21, 27–30 (1989).
- [9] W. H. Southwell, *Appl. Opt.* 18, 1240–1243 (1979).
- [10] J. H. McDermit and T. E. Horton, *Appl. Opt.* 13, 1444–1450 (1974).
- [11] P. W. Scott and W. H. Southwell, *Appl. Opt.* 20, 1606–1610 (1981).
- [12] C. C. Aleksoff, K. K. Ellis and B. D. Neagle, *Opt. Eng.* 30, 537–543 (1991).
- [13] Q. Zhan and J. R. Leger, *Opt. Exp.* 10, 324–331 (2002).

- [14] B. Hao and J. R. Leger, *Appl. Opt.* 46, 8211–8217 (2007).
- [15] J. R. Leger, G. J. Swanson and W. B. Veldkamp, *Appl. Opt.* 26, 4391–4399 (1987).
- [16] H. R. Wang, M. J. Cima, B. D. Kernan and E. M. Sachs, *J. Non-Cryst. Solids* 349, 360–367 (2004).
- [17] P. Sinai, *Appl. Opt.* 10, 99–104 (1971).
- [18] T. Schmidt, P. W. Oliveira, M. Mennig and H. K. Schmidt, *J. Non-Cryst. Solids* 353, 2826–2831 (2007).
- [19] D. R. Beltrami, J. D. Love, A. Durandet, A. Samoć, C. J. Cogswell, *Appl. Opt.* 36, 7143–7149 (1997).
- [20] M. I. Alayo, I. Pereyra, W. L. Scopel, M. C. A. Fantini, *Thin Solid Films* 402, 154–161 (2002).
- [21] Y. Asahara, H. Sakai, S. Shingaki, S. Ohmi, S. Nakayama et al., *Appl. Opt.* 24, 4312–4315 (1985).
- [22] R. Ashokan, R. Singh, V. Gopal and M. Anandan, *J. Appl. Phys.* 73, 3943–3950 (1993).
- [23] D. P. Hamblen, ‘Gradient Refractive Index Optical Lenses’, US Patent 3,486,808 (December 1969).
- [24] J. R. Hensier, ‘Method of Producing a Refractive Index Gradient in Glass’, US Patent 3,873,408 (25 March, 1975).
- [25] R. K. Mohr, J. A. Wilder, P. B. Macedo and P. K. Gupta, in ‘Technical Digest on Gradient-Index Optical Imaging Systems (Optical Society of America, Washington, DC, 1979)’, paper WA1.
- [26] M. Yamane, A. Yasumori, M. Iwasaki and K. Hayashi, *Proc. SPIE* 1328, 133–144 (1990).
- [27] T. M. Che, J. Brain, S. B. Caldwell and R. M. Mininni, *Proc. SPIE* 1328, 145–159 (1990).
- [28] N. Haun and D. T. Moore, *Appl. Opt.* 31, 5225–5229 (1992).
- [29] C. Wang and D. L. Shealy, *Appl. Opt.* 32, 4763–4769 (1993).
- [30] W. C. Elmore and M. A. Heald, ‘The Physics of Waves’ (Dover Publications, New York, 1985).
- [31] G. Beliakov and D. Y. C. Chan, *Appl. Opt.* 36, 5303–5309 (1997).
- [32] W. H. Southwell, *J. Opt. Soc. Am.* 72, 908–911 (1982).



Di Lin received a B.S. degree in Electrical Engineering from the University of Minnesota in 2004. He is currently working toward his PhD in Electrical Engineering at the University of Minnesota. His principal research interests include light propagation in inhomogeneous materials, laser cavity design and applications of volume holography.



James R. Leger received a B.S. degree in Applied Physics from the California Institute of Technology, Pasadena, in 1974, and a PhD degree in Electrical Engineering (Applied Physics) from the University of California, San Diego, in 1980. He worked for the 3M Company until 1984, when he joined the Massachusetts Institute of Technology (MIT) Lincoln

Laboratory, Lexington, as a Research Staff member. In 1991, he joined the faculty at the University of Minnesota, Minneapolis, where he is currently the Cymer Professor of Electrical and Computer Engineering and the Taylor Distinguished Professor. His principal research interests include laser design, applications of diffraction and advanced imaging systems. Dr. Leger received the Joseph Fraunhofer Award and the Robert M. Burley Prize from the Optical Society of America for advances in optical engineering in 1998. He is a fellow of the Optical Society of America (OSA), the International Society for Optical Engineers (SPIE), and the Institute of Electrical and Electronics Engineers (IEEE).